Formation, Structure, and Polymorphism of Novel Lowest-Dimensional AgI Nanoaggregates by Encapsulation in Carbon...

Stefano Leoni, Matteo Baldoni

Small

Related papers

Download a PDF Pack of the best related papers ⏷

Structure and Ionic Transport Properties of AgI 1− x Br x within Single-Wall Carbon Nanotubes…
I. Murin, Andrey Petrov

Computer simulation of ionic transport in silver iodide within carbon nanotubes
I. Murin, Andrey Petrov

Mechanics of filled carbon nanotubes
Paulo Cachim

Formation, Structure, and Polymorphism of Novel Lowest-Dimensional AgI Nanoaggregates by Encapsulation in Carbon Nanotubes**

*Matteo Baldoni, Stefano Leoni, Antonio Sgamellotti, Gotthard Seifert, and Francesco Mercuri**

The ability to encapsulate different materials has constituted one of the first applications of carbon nanotubes (CNTs). The pioneering work of Ajayan and Iijima[1] has been followed by several studies on this topic, leading to one of the most active fields of research concerning nanostructured materials.[2,3] Besides the possibility of creating intrinsically monodimensional materials through nanotube-driven template syntheses, one of the most interesting aspects of encapsulation concerns the formation of ordered structures in the hollow of CNTs, in the form of nanocrystallites, as often observed in experiments. The one-dimensional (1D) confined growth of different compounds has been viewed as a suitable route to the development of new low-dimensional materials, like nanowires. Moreover, the structure of the nanotube usually plays a crucial role in the growth process by selectively determining the stable atomic configuration of the filler.[2] As a result of the filling process, the properties of both the filler and the nanotube are generally different from their bulk and pristine forms, respectively.

In recent experimental studies, metal halides were inserted into the nanotube hollow with excellent yield.[4–6] In particular, Bendall et al. demonstrated the encapsulation of silver iodide (AgI) into CNTs with diameters as small as

[*] Prof. A. Sgamellotti, Dr. F. Mercuri
    ISTM-CNR and Department of Chemistry
    University of Perugia
    06123 Perugia (Italy)
    Fax: (+49) 351-4646-3002
    E-mail: merc@thch.unipg.it

    M. Baldoni
    Department of Chemistry
    University of Perugia
    06123 Perugia (Italy)

    Dr. S. Leoni, Dr. F. Mercuri
    Max-Planck-Institut für Chemische Physik fester Stoffe
    01187 Dresden (Germany)

    M. Baldoni, Prof. G. Seifert
    Fachbereich Chemie, Technische Universität
    Dresden 01062 Dresden (Germany)

1 nm.[4] The filling process for small-diameter nanotubes induces a structural deformation of the sidewall, which, in turn, modifies the nanotube properties. Notably, the same authors related the observed changes to barely structural factors, owing to the nonbonding interactions between d^{10} guest metal ions and the carbon atoms on the sidewall.[4] The most significant structural deformation is found in small-diameter AgI-filled nanotubes in form of an ovalization of the nanotube section. The deformation of the CNTs induced by filling and the resulting valence orbital rehybridization can be expected to induce remarkable changes in their reactivity.

However, due to intrinsic difficulties in the experimental characterization of nanostructured materials, many microscopic details of the filling process and of the resulting structures remain, to a large extent, still unclear. In contrast to experimental observations, computer simulation methods, in particular molecular dynamic (MD) simulations, represent an ideal tool for the investigation of reactions at the atomic level. In this respect, the computational studies carried out by Wilson et al. during the past few years provided a fundamental approach to the field.[7–11] In particular, Wilson focused on the structural and dynamical aspects concerning the behavior of model systems[7,8] or KI crystallites[9,10] confined by rigid CNTs.

In this work, we perform MD simulations on the formation, stability and structure of AgI nanocrystallites encapsulated into single-walled (SW) (*n*,*n*) CNTs of different diameters. Motivated by the experimental evidence cited above[4] and by theoretical predictions[7] we adopt flexible CNT models able to account for the deformation of the sidewall upon filling, thus proceeding a step further with respect to previous simulations.

For the confined crystallization of AgI into CNTs we used two strategies: direct insertion of AgI clusters (ranging from 64 to 124 atoms) into (*n*,*n*) CNTs of finite length (*n* = 8–10), and diffusion of ions into CNTs from a bath of liquid AgI. The diameter range of the chosen CNT system is of the order of that observed in encapsulation experiments for AgI.[4] The rigid-ion interaction potential of Parrinello et al.[12] was used for AgI. The potential was developed in accordance with the (α–β) phase transition in AgI and has proven very reliable over a broad range of temperatures and pressures,[13] both in the bulk and for small clusters.[14] The nanotubes were described with the flexible potential of Walther et al.,[15] including terms for bonded (stretching, bending, torsion) and nonbonded (Lennard–Jones, LJ) interactions, thus providing a realistic picture of the structure of the sidewall and of its possible modifications upon filling. The ion–nanotube interactions were accounted for with a LJ potential with parameters derived from the atom/graphite values corresponding to the closed-shell neutral isoelectronic counterparts. For Ag$^+$/C, literature parameters for Pd/C[16] were taken, whereas for I$^-$/C the values suggested by Wilson, based on Kr/C parameters, were employed.[10] In the MD simulations of finite systems the equations of motion were integrated in the canonical ensemble using a time step of 2 fs. For periodic systems an isothermal–isobar-

ic ensemble was used .[17] Long-range electrostatic interactions were treated with Ewald summation.

In a first set of simulations, sections of suitable diameter were recut from equilibrated bulk structures and subsequently inserted into the hollow of CNTs, previously equilibrated at room temperature. Sectioning was performed along crystallographic directions (e.g., [100] in NaCl, or [001] in wurtzite-type structures) in order to produce charge-neutral clusters of composition $(AgI)_n$. As bulk structures we considered the hexagonal β phase of wurtzite-type structure,[18] which is stable at ambient conditions, and the high-pressure polymorph of rocksalt-type structure (NaCl type).[19,20] In fact, the latter may become relevant in confined situations in which additional pressure is applied on the guest aggregates by the CNT walls. The size of the CNT models was chosen with an approximate length ratio of 1:1 between the filled part of the nanotube and the unfilled edges. This resulted in approximate CNT lengths ranging from 15 to 20 nm. The AgI-filled systems were equilibrated at 300 K and propagated for 400 ps in the canonical ensemble. In all simulations, the AgI clusters underwent sensible structural rearrangements irrespective of the initial (wurtzite or rocksalt) structure, converging to similar configurations in both cases. Hereafter we will only discuss structures originating from clusters recut from the rocksalt structure. Configurations obtained from initial clusters of β structure are given in the Supporting Information for comparison. All equilibrated structures of AgI clusters encapsulated into (n,n) CNT models of different radii ($n=8–10$) exhibit structural order, as shown in Figures 1 and 2, and will be hereafter discussed in detail.

The insertion of an $(AgI)_{32}$ cluster, initially cut as a 2×2 (Ag_2I_2) square-section parallelepiped (cut parallel to [100] directions in NaCl), into the cavity of a (8,8) CNT and the subsequent thermal equilibration led to the formation of an unprecedented lowest-dimensional crystal structure. In contrast with the initial configuration, the relaxed structure exhibits a monodimensional (2×1) section along the nanotube axis, giving rise to a ribbonlike lattice with long and short connections (see Figure 1a), comparable to the atomic arrangement in (110) planes of the rocksalt structure. By extending the (n,m) index nomenclature usually applied to CNTs,[21] this structure corresponds formally to a (1,1) nanotube fragment with alternating silver and iodine atoms on the CNT hexagonal net. The narrow diameter of (8,8) nanotubes does not allow to accommodate crystal structures with a 2D transversal section. In contrast, the formation of the AgI nanoribbon induces a remarkable deformation of the sidewall, as shown in Figure 1a (right panel). Moreover, the 2×1 AgI wire is twisted along the CNT axis (Figure 1a, bottom panel), giving rise to a helical propagation of the distorted nanotube cross section, similar to CoI_2-filled CNTs.[6] Although there is no strict one-to-one correspondence between the atomic positions of the guest aggregate and the sidewall carbon atoms sites, the CNT deformation propagates commensurably with the twist of the internal ribbon. For the encapsulated structure, the low coordination number of Ag and I is only partially amended by the helicity of the ribbon along the CNT axis. Hence, an additional
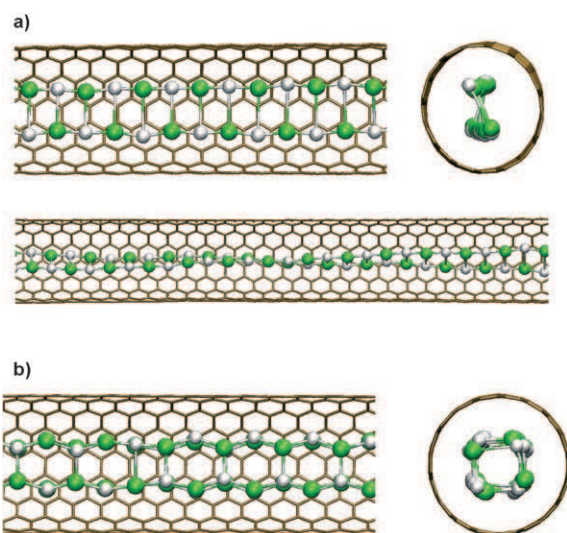

Figure 1. Snapshots from the MD simulation at 300 K of an AgI cluster a) encapsulated in a (8,8) CNT; b) encapsulated in a (9,9) CNT. Silver and iodine ions are shown as white and green spheres, respectively.
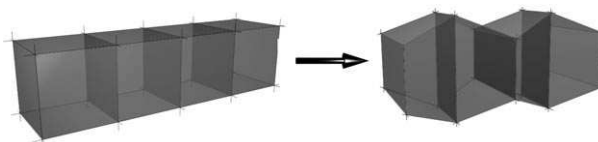

Figure 2. Schematic image of the geometrical transformation leading from a cubic (rocksalt-like) structure to a nanotube-like arrangement. In the final state, the occurrence of hexagonal patterns is observed.

means to achieve a denser local packing is the flattening of the CNT sidewalls towards the ribbon surface. The chemical interactions are thus retuned to stabilize the whole system. This finding confirms the experimental evidence[4] on the deformation of the CNT cross section upon filling with AgI for nanotube diameters of around 1 nm, and is thus consistent with the size of the (8,8) model. This result also underlines the importance of using flexible CNT models to simulate the filling process, pinpointing the active role of the container to stabilize lower-dimensional structures that are not limited to the bare confining function.

In the following a larger $(AgI)_{66}$ cluster was placed into the hollow of a (9,9) CNT. Relaxation of this system led to a new configuration with a 2D cross section, in contrast with the 1D case of the (8,8) nanotube. Its structure (Figure 1b) is the one of a folded (CNT-like) hexagonal sheet of alternating Ag and I ions and corresponds to an armchair (2,2) AgI inorganic nanotube. The larger (9,9) CNT diameter allows for more space for accommodating an ordered structure and the cross section of the crystallite is 2D. Owing to the reduced anisotropy of the crystal cross section (Figure 1b) the filled (9,9) CNT stays cylindrical. The equilibrium configurations result from the initial cubic motifs of NaCl structure type by distorting the square cross sections along directions perpendicular to the nanotube axis, as de-

picted in Figure 2. This results in an arrangement of alternating rectangular Ag_2I_2 units rotated relative to each other by 90°. The alternance of hexagonal and square motifs is common in binary systems based on tetrahedral structures. Apart from AgI, chalcogenides of the copper group like CdSe or main group pentelides crystallize in the wurtzite or sphalerite structure types, and also transform into the rocksalt type under pressure.[22] Intermediate structures often display a coordination in between, exhibiting compressed six-ring or skew cubes. In confined systems the sequence is reversed with small tubes favoring the formation of compact structures consisting of square-cubic motifs, with the appearance of six rings on enlarging the tube diameter. In this respect, the structure crystallized inside the (9,9) CNT represents an intermediate packing situation. The distorted hexagonal motifs are sometimes spaced by defects containing AgI four and eight rings (Figure 1b, left panel).

For encapsulation into a (10,10) CNT, the internal cavity was large enough for different starting AgI cluster sizes to be considered. This offered the opportunity to investigate the dependence of the final crystallite morphology on the initial conditions. The total number of inserted atoms was kept constant, while the way of occupying the internal volume was modified. To this end, AgI nanorods carved from rocksalt with 2×2 or 3×3 cross sections were inserted into the nanotube. Both initial clusters exhibit some form of mismatch within the nanotube. The 2×2 nanorod is elongated and consequently locally less dense. The 3×3 rod is shorter and locally very close to the internal surface of the CNT. Both initial clusters evolve, at 300 K, towards intermediate aggregates of similar density, the former by shortening, the latter on expanding along the CNT axis. However, they result into distinct equilibrium structures.

The system evolved from the 2×2 nanorod crystallizes into a (4,0) AgI nanotube (see Figure 3a). In contrast with the case of encapsulation into a (9,9) CNT, the AgI nanotube is larger and rolled according to chiral vectors corresponding to a zigzag sidewall. The pseudo-octagonal section

of the confined AgI lattice does not cause ovalization of the nanotube shape, as shown in Figure 3a (right panel). Also, in this case, lattice defects with four- and eight-ring motifs do form during crystallization, as shown in the snapshot of Figure 3a (left panel). In contrast, the equilibration started from a 3×3 cross-section nanorod converged to a AgI configuration formally equivalent to a chiral (4,2) nanotube (see Figure 3b). The AgI nanotube exhibits a quasicircular, decagonal cross section that leaves the CNT cross section practically undeformed. Notably, the same structure is obtained from a starting cluster of wurtzite structure (cut along the [001] direction) owing to a similar initial AgI linear density (see Supporting Information).

The emerging polymorphism suggests on the one hand different ways to novel forms of aggregation in the nanoregime. On the other hand, it hints at concurring factors in the formation of crystallites within CNTs. Encapsulated AgI nanotubes with a larger diameter can grow if the additional energy costs caused by a larger surface area are compensated by the lowering of the chemical potential, associated with a denser packing. The (4,0) AgI nanotube is thinner and less dense, whereas the (4,2) nanotube has a larger cross section but is more compact. The interplay of these two factors should allow for several free-energy local minima, corresponding to possible metastable phases that can be quenched by encapsulation.

All geometries were optimized by simulated annealing (warming above 500 K, cooling at a rate of $-0.1 \, K \, ps^{-1}$) and the final structures are shown in Figure 4. The optimized structures of the four AgI-CNT systems discussed above exhibit essentially the same features as of their counterparts equilibrated at room temperature, shown in Figures 1 and 3. The confined AgI clusters are arranged in regular CNT-like (n,m) geometries with a characteristic silver iodide bond length of between 2.74 and 2.81 Å (see Figure 4b–d), with the exception of the (8,8) CNT, in which the Ag-I distance shrinks to 2.60 Å (Figure 4a). The structure of the optimized AgI-filled (8,8) CNT is also twisted but to a lesser extent with respect to the system equilibrated at 300 K. Moreover, the annealing procedure confirmed the presence of structural defects (left side of Figure 4c) and competing structures (right side of Figure 4b) based on the alternation of hexagonal and squared patterns.

The dynamics of the formation of CNT-confined AgI structures was also investigated by simulating the filling process from the immersion of a nanotube in a bath of molten silver iodide. Only (8,8) and (9,9) CNTs were considered, since they account for both two- and three-dimensional confined crystal structures. A simulation setup similar to that implemented by Wilson et al.[7–11] was used. A $35 \times 35 \times 57 \, Å^3$ box of molten AgI was initially equilibrated for 800 ps at 1000 K. A sufficiently large cylindrical region of AgI was removed from the melt and substituted by initially capped (8,8) or (9,9) CNTs. As the filling process depends less critically on nanotube edge effects, the calculations were carried out with shorter CNTs, consisting of 288 and 324 carbon atoms for the (8,8) and (9,9) systems, respectively. After an additional equilibration time of around 600 ps at 1000 K the CNT caps were removed. A filling time ranging from 20 to
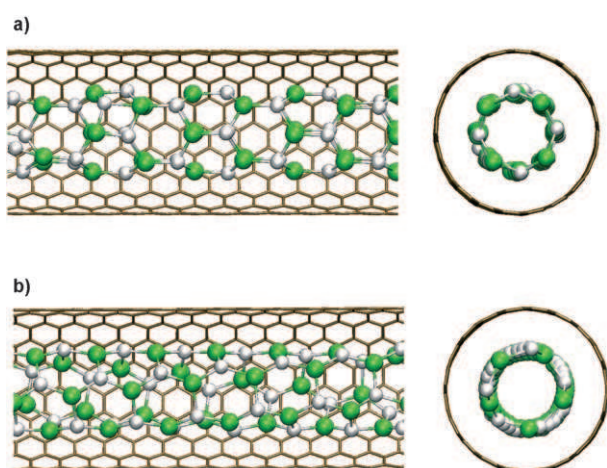

Figure 3. Snapshots from the MD simulation at 300 K of AgI encapsulated in a (10,10) CNT starting from a) a 2×2 cross section AgI cluster and b) a 3×3 cross section AgI cluster. Silver and iodine ions are shown as white and green spheres, respectively.
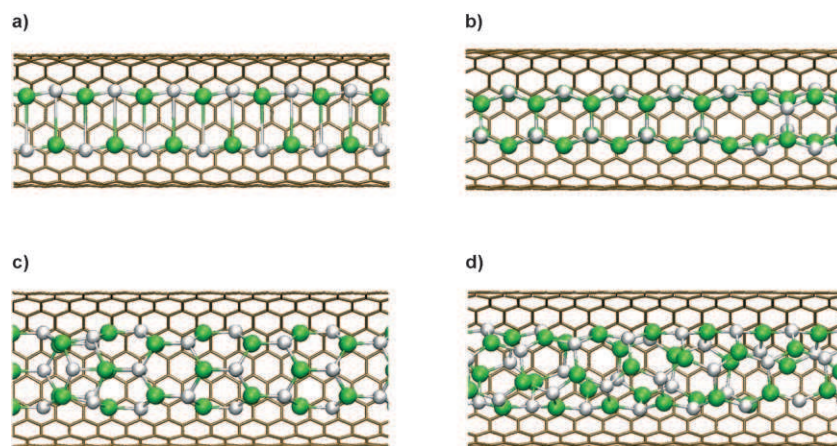
Figure 4. Optimized geometry of an AgI cluster encapsulated in a) an (8,8) CNT, starting from a 2 × 2 section of an equilibrated rocksalt structure; b) a (9,9) CNT, starting from a 2 × 2 section of an equilibrated rocksalt structure; c) a (10,10) CNT, starting from a 2 × 2 section of an equilibrated rocksalt structure, and d) a (10,10) CNT, starting from a 3 × 3 section of an equilibrated rocksalt structure. Silver and iodine ions are shown as white and green spheres, respectively.

and stability at room temperature and are formed spontaneously by immersion of open-end CNTs into molten AgI. All crystal structures are formally (n,m) AgI nanotubes with chiral vectors n and m depending on the CNT diameter and on the local environment. Confined growth in very small diameter CNTs, such as the (8,8) nanotube, gives rise to ribbonlike AgI arrangements. This configuration—a lower-limiting case for formation of AgI ordered structures into the hollow of CNTs—exhibits a significant deformation of the nanotube shape.

Slightly larger diameter CNTs, such as the (9,9) and (10,10) CNTs, allow the confined growth of AgI structures with 2D cross sections. This finding agrees with experimental observations that indicate pseudocircular sections of encapsulated AgI crystallites for CNT diameters larger or equal to 1.15 nm. Moreover, the filling of large-diameter CNTs can eventually lead to the concurrent formation of different AgI aggregates, depending on the nanotube diameter and on environmental factors such as local instantaneous
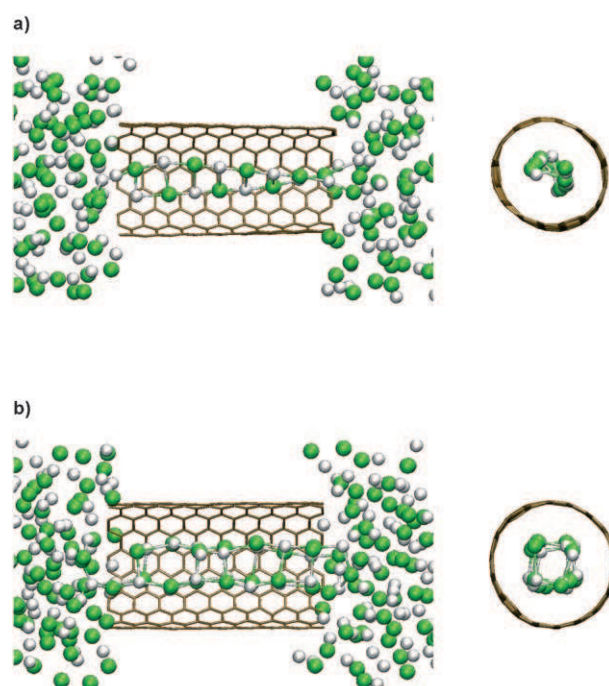
40 ps was observed, after which the system was equilibrated for at least 100 ps.

The dynamical evolution of the filling process for (8,8) and (9,9) CNTs is illustrated by movies included as Supporting Information. The initial steps of the filling of (8,8) and (9,9) nanotubes share mechanistic similarities. Silver and iodine ions enter the CNT from both ends in the form of Ag-I linear chains, as also observed in Reference [7]. The relaxation towards the final configurations begins when the two chains come closer to each other. Representative snapshots of the equilibrated CNT-filled systems are shown in Figure 5.

In the case of the (8,8) CNT, typical configurations (see Figure 5a) correspond to the arrangement obtained from relaxing nanorods recut from bulk structures inside the CNTs. In particular, the formation of a 2×1 Ag-I twisted nanoribbon is confirmed. The latter forms from AgI filaments approaching each other from opposite tube ends. No alternative structures appear. The ovalization of the CNT takes place while the nanoribbon is formed, underlying the active role of the CNT in the stabilization of the forming guest aggregate.

The filling of the (9,9) CNT results in a confined crystal structure with 2×2 cross section (Figure 5b) reproducing the (2,2) nanotube found from relaxing clusters derived from bulk structural motifs, as described above. The nanotube shape is practically undeformed during and upon filling (see Figure 5b, right). However, the dynamics of the filled (9,9) CNT exhibit an intense interplay between AgI structures based on square and hexagonal patterns. Indeed, the high temperature facilitates the processes, as sketched in Figure 2, leading to the coexistence of different structural (stable and metastable) AgI phases in nanometer-sized regions of space.

In summary, MD simulations provided clear evidence for novel silver iodide phases upon confinement in small-diameter SWCNTs. Such structures exhibit remarkable order

Figure 5. a) Snapshot from the MD simulation of the filling of a) an (8,8) CNT inserted in a bath of melt AgI at 1000 K, and b) a (9,9) CNT inserted in a bath of melt AgI at 1000 K. Silver and iodine ions are shown as white and green spheres, respectively. Only a relevant part of the AgI bath exterior to the nanotube is shown, for clarity.

pressure. Interfaces between different confined AgI nano-crystallites are likely to be observed, as well as a variety of defective structures. Indeed, the interplay between different stable and metastable phases is observed in the course of MD simulations on the encapsulation of AgI from the melt into a (9,9) CNT. Work is ongoing to assess the detailed dynamics of the filling process and the properties of the resulting encapsulated crystal nanowires in different environmental and growth conditions.

[1] P. M. Ajayan, S. Iijima, *Nature* **1993**, *361*, 333.

[2] R. R. Meyer, J. Sloan, R. E. Dunin-Borkowski, A. I. Kirkland, M. C. Novotny, S. R. Bailey, J. L. Hutchinson, M. L. H. Green, *Science* **2000**, *289*, 1324.

[3] a) Y. N. Xia, P. D. Yang, Y. G. Sun, Y. Y. Wu, B. Mayers, B. Gates, Y. D. Yin, F. Kim, Y. Q. Yan, *Adv. Mater.* **2003**, *15*, 353; b) W. Q. Han, S. S. Fan, Q. Q. Li, Y. D. Hu, *Science* **1997**, *277*, 1287; c) G. Hummer, J. C. Rasaiah, J. P. Noworyta, *Nature* **2001**, *414*, 188; d) K. Koga, G. T. Gao, H. Tanaka, X. C. Zeng, *Nature* **2001**, *412* 802.

[4] J. S. Bendall, A. Ilie, M. E. Welland, J. Sloan, M. L. H. Green, *J. Phys. Chem. B* **2006**, *110*, 6569.

[5] a) J. Sloan, M. Terrones, S. Nufer, S. Friedrichs, S. R. Bailey, H. G. Woo, M. Rühle, J. L. Hutchinson, M. L. H. Green, *J. Am. Chem. Soc.* **2002**, *124*, 2117; b) J. Sloan, D. M. Wright, H. G. Woo, S. Bailey, G. Brown, A. P. E. York, K. S. Coleman, J. L. Hutch-inson, M. L. H. Green, *Chem. Commun.* **1999**, 699; c) E. Flahaut, J. Sloan, S. Friedrichs, A. I. Kirkland, K. S. Coleman, V. C. Williams, N. Hanson, J. L. Hutchison, M. L. H. Green, *Chem. Mater.* **2006**, *18*, 2059; d) A. Ilie, J. S. Bendall, D. Roy, E. Philp, M. L. H. Green, *J. Phys. Chem. B* **2006**, *110*, 13 848.

[6] E. Philp, J. Sloan, A. I. Kirkland, R. R. Meyer, S. Friedrichs, J. L. Hutchinson, M. L. H. Green, *Nat. Mater.* **2003**, *2*, 788.

[7] M. Wilson, *J. Chem. Phys.* **2006**, *124*, 124 706.

[8] M. Wilson, *Nano Lett.* **2004**, *4*, 299.

[9] a) M. Wilson, *J. Chem. Phys.* **2002**, *116*, 3027; b) M. Wilson, *Chem. Phys. Lett.* **2004**, *397*, 340; c) M. Wilson, *Chem. Phys. Lett.* **2002**, *366*, 504.

[10] M. Wilson, P. A. Madden, *J. Am. Chem. Soc.* **2001**, *123*, 2101.

[11] M. Wilson, S. Friedrichs, *Acta Crystallogr. Sect. A* **2006**, *A62*, 287.

[12] M. Parrinello, A. Rahman, P. Vashishta, *Phys. Rev. Lett.* **1983**, *50*, 1073.

[13] J. Tallon, *Phys. Rev. Lett.* **1986**, *57*, 2427.

[14] A. Wootton, P. Harrowell, *J. Phys. Chem. B* **2004**, *108*, 8412.

[15] J. H. Walther, R. Jaffe, T. Halicioglu, P. Koumoutsakos, *J. Phys. Chem. B* **2001**, *105*, 9980.

[16] S. K. R. S. Sankaranarayanan, V. R. Bhethanabotla, B. Joseph, *Phys. Rev. B* **2005**, *72*, 195 405.

[17] S. Melchionna, G. Ciccotti, B. L. Holian, *Mol. Phys.* **1993**, *78*, 533.

[18] A. F. Wright, B. E. F. Fender, *J. Phys. Soc. Jpn.* **1977**, *9*, 295.

[19] S. Hull, D. A. Keen, *Phys. Rev. B* **1999**, *59*, 750.

[20] R. C. Hanson, T. A. Fjedly, H. D. Hochheimer, *Phys. Status Solidi B* **1975**, *70*, 567.

[21] R. Saito, G. Dresselhaus, M. S. Dresselhaus, *Physical Properties of Carbon Nanotubes*, Imperial College Press, London, **1998**.

[22] A. Mujica, A. Rubio, A. Muñoz, R. J. Needs, *Rev. Mod. Phys.* **2003**, *75*, 863.